

S. Legutke · E. Maier-Reimer

The impact of a downslope water-transport parametrization in a global ocean general circulation model

Received: 15 August 2000 / Accepted: 13 September 2001 / Published online: 4 January 2002
© Springer-Verlag 2002

Abstract The impact of a downslope water-transport parametrization on the circulation and water mass characteristics of a global depth-level ocean general circulation model is investigated. The spreading of dense water from the formation regions into the deep ocean is known to be poorly represented in depth-level models with no bottom boundary layer resolved or attached. The new scheme is simple and intends to parametrize the effects of various oceanographic processes (rather than the processes themselves) that help dense water to descend topographic slopes by which the formation regions are separated from the world ocean. The new scheme significantly improves the large scale properties of the North Atlantic Deep Water. Changes in the North Atlantic circulation, however, are rather small. In the Southern Ocean, the exchange between the dense water formation regions on the continental shelves and the deep ocean is strengthened at the expense of deep water mass formation by open ocean convection. In all three ocean basins, the density of the deep and bottom water is higher with the new parametrization, which brings the simulations closer to observations in the Atlantic and Indian Oceans. In the Pacific Ocean, however, where the density has already been well reproduced without the downslope transport, it becomes slightly too high. The results are in agreement with those from other model studies.

1 Introduction

The densest water masses in the world ocean are formed in semi-enclosed basins separated from the abyssal seas by steep continental slopes or submarine ridges. In order

to contribute to the ventilation of the deep ocean, the dense water has to descend the slopes or to flow over the ridges.

In the Southern Hemisphere, the most important dense water formation regions are the Antarctic continental shelves. Densification of surface water there occurs through cooling either by the atmosphere or by melting of ice shelves, and through increase of salinity by release of brine during the formation of sea-ice. Downslope flow of dense shelf water has been observed in the Weddell and Ross seas, and traces of such flow have been found all along the Indian Ocean sector of the Antarctic shelves (Baines and Condie 1998). When the water flows down the slope, it mixes with the overlying warmer and saltier Circumpolar Deep Water (CDW) (Foster and Carmack 1976). The mixing product, the Antarctic Bottom Water (AABW), ventilates the abyss of the world ocean (Luyten et al. 1993; Rintoul 1998).

The source water of CDW, the North Atlantic Deep Water (NADW), is also a product of mixing processes which involve dense bottom water flowing down the steep topographic slopes of the Greenland-Scotland ridge system. This overflow water mixes with overlying water masses, in particular with Labrador Sea water (Dickson and Brown 1994), but derivatives of AABW and of saline water of Mediterranean origin contribute as well (Rhein and Hinrichsen 1993). The latter again contain a dense slope water mass, the Mediterranean outflow (Price et al. 1993), which, in addition, helps to precondition the Atlantic inflow to the Arctic Ocean for deep water formation (Reid 1979).

Although it has been argued that cold brine-enriched shelf water must transport salt into the deep Arctic Ocean to explain the high salinity there (Aagaard et al. 1985), formation of dense deep or bottom water at high northern latitudes is much less evident. Schauer et al. (1997) see the reason in the more efficient dilution of Arctic shelf water by continental runoff.

The layer thickness of observed downslope flow is O (10 m) to O (100 m) and the flow is often intermittent in

S. Legutke (✉) · E. Maier-Reimer
Max-Planck-Institut für Meteorologie Bundesstraße 55,
20146 Hamburg, Germany
E-mail: legutke@dkrz.de

time (Dickson and Brown 1994). Thus, direct observations of the descent of dense water are rare, and most of our knowledge about the dynamics of downslope flow has been deduced from high-resolution regional or idealized numerical ocean models, or from laboratory experiments. Price and O'Neil Baringer (1994) examined the outflow from the Mediterranean Sea, the Filchner Ice Shelf, and the Greenland-Norwegian seas. They note in particular that the density ordering of the source water masses is the reverse of the density ordering of the final products. Price and O'Neil Baringer (1994) conclude that entrainment of ambient water into the bottom layer varies considerably between the different regions.

In their simulation of bottom flow with stream-tube models, Price and O'Neil Baringer (1994) considered entrainment in the dynamics of the stream by making it dependent on the density difference between the bottom water and the ambient water, the thickness of the bottom layer, and its velocity. Using the appropriate parameters for each of the outflow regimes, they were able to simulate the main characteristics of the flow. Crucial parameters for the entrainment in their models are the local bottom slope, which is scale-dependent, and the bottom drag coefficient, which is assumed to depend on the surface roughness.

Baines and Condie (1998) summarize the results of recent modelling activities with high-resolution 3D-models. These models show that the frontal currents which evolve by the geostrophic adjustment process after convective formation of dense water can be extremely unstable. Offshore transport of dense water is controlled by baroclinic eddies which accompany the adjustment process. In addition, downslope Ekman drainage from the dense bottom layer may cause eddies to form by vortex stretching of the water column above the dense layer. The relative importance of downslope transport by eddies or by Ekman flow depends on the ratio of the Ekman layer depth and the depth of the dense layer. Baines and Condie (1998) showed that flow characteristics can change in the downstream direction by detrainment and entrainment, local changes in bottom topography and bottom roughness, as well as by changes of the strength of the dense water source.

The downslope transport increases when the models include small-scale canyons cutting through the shelf slope. These canyons may accelerate the descent of the dense water by geostrophically channelling the fluid downslope (Jungclaus and Mellor 1999). On the other hand, the fluid may find its level of neutral density at a higher level due to the increased velocity and associated larger entrainment rates.

Ocean general circulation models (OGCMs) that have their levels of computation at horizontal surfaces, depth-coordinate or z-level models as they are called, are widely used in coupled climate models. Since these models normally do not resolve the processes which control downslope flow (e.g. baroclinic eddies, Ekman layer dynamics), dense water, which is formed on shelves, tends to stay there instead of flowing downslope.

Downslope transport of dense water in z-level models is described as a stepwise procedure of alternating horizontal and vertical diffusive or advective transports. There may be an additional downward transport by convective adjustment, used to remove hydrostatic instabilities. Dense water that descends a slope thus undergoes strong dilution with lighter water found offshore. The deep and bottom water in depth-coordinate models is thus often too light (Campin and Goosse 1999; Danabasoglu and McWilliams 1995), which has severe consequences for the ventilation of the deep ocean. A frequently used remedy to this problem is to artificially increase the density of the water in the formation regions above observed values, so that even with a too strong mixing with lighter water, the descending water has about the right density when it arrives at the bottom (Toggweiler and Samuels 1995; England 1993). This approach, however, is not appropriate in climate change studies, where the prediction of surface conditions in dense-water formation regions is an essential prerequisite for a prediction of ventilation changes in the deep ocean and thus of the long-term response of the climate system.

The sensitivity of this response to the formulation of the downslope transport of tracers might be large, as suggested by the study of Lohmann (1998) with an idealized model of the Atlantic Ocean coupled to an energy-balance model of the atmosphere. Lohmann (1998) added a 'slope convection' term to the tracer transport equations of the grid cells nearest to the bottom, as was proposed by Beckmann and Döscher (1997). He showed that the sensitivity of the thermohaline circulation of the coupled system to a perturbation of the surface salinity south of the Greenland-Scotland ridge system was reduced with the 'slope convection' included. Improvement of the downslope transport in depth-coordinate ocean models is therefore needed in order to increase their reliability in climate studies.

Killworth and Edwards (1999) implemented a bottom boundary layer (bbl) with spatially and temporarily changing height, including entrainment and detrainment into a depth-coordinate ocean model. Since the bbl is based on the full standard Boussinesq Navier-Stokes equations with the pressure gradients formulated within the bottom layer, the finite-difference formulation invokes pressure-gradient errors of the kind known from terrain-following σ -coordinate models.

A similar bbl model, which allows temporal and spatial variations of the bbl height, has been implemented by Song and Chao (2000) into the MOM OGCM. For high resolution test cases in idealized ocean basins, both models produced significant downslope flow, while in the corresponding models with no bbl, the dense water was trapped in the shallow part of the basin.

With the formulation of Killworth and Edwards (1999) and Song and Chao (2000), problems can arise when the simulated height of the bottom layer becomes larger than half of the bottom cell. In global OGCMs, this is most likely to occur in regions with shallow sill

depths, since the vertical resolution is commonly specified to be higher in the upper ocean in order to account for the larger vertical variations in density there. OGCMs used in climate studies have a layer thickness of $O(10\text{ m})$ in the upper ocean. In the model used in this study, most of the changes due to the bbl occur in 600 to 1000 m depth (see e.g. Fig. 2) where the layer thickness is 200 m. The sill depth of the Strait of Gibraltar is at 400 m with a layer thickness of ca. 100 m.

Gnanadesikan (unpublished) tested a similar formulation of a bbl, however, by disallowing the height of the bottom cell to vary in time or space, he avoided potential problems of the bottom layer becoming too thick. With a pre-specified layer thickness, turbulence is modelled with a turbulence coefficient rather than with de/entrainment. This model also satisfactorily treated downslope flow in idealized test cases. Sensitivity studies of the influence of the specified bbl height, however, showed a rather large impact of this parameter on the model results.

Beckmann and Döscher (1997) avoided the problems with the horizontal pressure-gradient errors in terrain-following bbl-coordinates by only calculating tracer tendencies in the bbl. The velocities and tracer distribution entering these equations are calculated in depth-coordinates. This requires the bottom layer to fill the whole grid cell above the bottom. The coupling to the interior cells is done by using a weighted average of the tracer tendencies calculated in depth-coordinates and those calculated in the bbl. With this model, Beckmann and Döscher (1997) showed that a coarse-resolution version with bbl formulation simulated dense plumes on a sloping bottom with shape and path similar to those in a higher-resolution version with no bbl and to those in a σ -coordinate model version. Since in global OGCM used in climate studies, velocities near the bottom are rather weak due to their coarse resolution, Beckmann and Döscher (1997) also run a test case where only diffusion in bbl coordinates was activated. The diffusion coefficient was different from zero only when the condition for 'slope convection' was fulfilled, i.e. when the upper bottom cell contained the denser water. Even with this purely diffusive bbl formulation, a more realistic spreading of plumes above bottom slopes was obtained.

These mentioned bbl parametrizations have only been implemented in idealized ocean basins or high resolution regional models (Dengg et al. unpublished). Nurser et al. (unpublished) have reported on a 10 year simulation with an improved Killworth and Edwards (1999) bbl implemented in a global 1° ocean model. However, this integration was too short to allow conclusion about the impact of the bbl on the model climate.

The first description of the impact of a bbl parametrization in a long-term run of a global OGCM with realistic topography is given by Campin and Goosse (1999). As in Beckmann and Döscher (1997), they consider the entire bottom cell to constitute the bbl and

modify only tracer tendencies. Downslope velocity is not taken from the basic model, however, but is calculated from a balance between the downslope pressure gradient (on horizontal surfaces) and a linear bottom drag. A compensating flow is specified to occur immediately above the lower bottom cell involved in the mixing.

Here we describe the impact of a downslope tracer transport scheme in another global OGCM with realistic topography. The parametrization is similar to the 'slope convection' case described by Beckmann and Döscher (1997). As in that of Campin and Goosse (1999), the whole bottom cell belongs to the bbl. It differs from their formulation in that the transport is considered to be a directional turbulent exchange. The implementation is similar to the vertical convective adjustment used in OGCMs, and thus no additional tuning parameter is introduced. The rationale behind the search for a parametrization as simple as possible, which however helps to improve the deep water properties in global OGCMs, is that most of the mentioned processes which influence downslope transport are not resolved in OGCMs. We do not aim at parametrizing any of these processes, but rather their overall effect on the large-scale water mass properties. In other words we hope to improve the deep ocean stratification and circulation by reducing the dilution of deep dense water on its downslope descent and by increasing the strength of the exchange between the formation regions and the deep ocean. The model has a somewhat finer resolution than that of Campin and Goosse (1999). It differs in many other aspects as well, the main difference being the incorporation of a fully prognostic sea-ice model and the forcing with high-frequency instead of annual-mean data. This allows to explicitly simulate the formation of dense water at the surface instead of artificially increasing the surface density. The model, the bbl parametrization, and the experiment setup is described in the next section. The climatological state of the ocean simulated with and without the bbl parametrization are compared in Sect. 3. Conclusions and a summary are given in Sect. 4.

2 Description of the ocean model and the experiment

The model used in the present study is a global version of the Hamburg Ocean Primitive Equation GCM (HOPE-G). Variants of the model have been used in studies of the global ocean general circulation (Drijfhout et al. 1997; Stössel and Kim 1998), in regional studies (Legutke 1991; Marsland and Wolff 2000), and in studies of the coupled atmosphere-ocean system (Frey et al. 1997). Simulations with the present model version are presented in Legutke et al. (1997) and Legutke and Maier-Reimer (1999). The numerical model formulation is described in detail in Wolff et al. (1997). The model equations are discretized on a Gaussian grid ($T42$, ca. 2.8°) with additional refinement in the meridional direction on both sides of the equator, and on 20 horizontal surfaces at 10, 30, 51, 75, 100, 125, 150, 175, 206, 250, 313, 425, 600, 800, 1050, 1450, 2100, 3000, 4000, 5250 m. The concentration of the model levels in the upper ocean serves to improve the representation of the highly variable thermocline, in particular in the tropical oceans. A good resolution of the topography is guaranteed despite the large distances between levels at large depths, since the model discreti-

zation allows for partial vertical grid cells at the bottom (see e.g. Fig. 3). Thereby, the resolution of the bottom topography is limited by the horizontal resolution of the grid only, and not by the number of computational levels. The baroclinic pressure is always computed at a constant depth for each layer, and thus does not induce spurious bottom-pressure terms (see Wolff et al. Fig. 2). It has been shown that this formulation gives a smoother flow field above topographic features than models with a comparable number of layers and full vertical cells (Adcroft et al. 1997).

The model domain includes the Mediterranean Sea, as well as the Hudson and Baffin bays, and the Baltic Sea. The Arctic Ocean is connected to the Pacific by the Bering Strait, and to the Atlantic by the Denmark Strait and the Iceland-Scotland passages. Small-scale features, as e.g. eddies, are not resolved in the straits or in other parts of the model domain. Their effect on the large scale circulation is parametrized by assuming vertical and horizontal 'eddy' diffusion and viscosity coefficients which depend on the density stratification and the velocity shear. Near the bottom, a linear Rayleigh friction is included, in addition to increased vertical eddy viscosities and no-slip conditions (the latter is applied at all solid boundaries). At the surface, a turbulent deepening of the mixed-layer is parametrized by increasing the vertical eddy diffusivity and viscosity coefficients when the density stratification becomes weak. Hydrostatic instabilities are removed by homogenization of the unstable part of the water column, the convective adjustment. Convection occurs most frequently in high latitudes, where it is triggered by surface cooling or increase of surface salinity due to sea-ice formation (Figs. 1 and 5).

As usual in z-level models, the transport of tracers in the default version is purely horizontal or vertical. Thus, dense bottom water descending a slope is diluted with light ambient water to a larger extent than seems appropriate, and the deep water is too light (Figs. 2c, 9a,c).

This problem is common to many other efforts of simulating the climate of the world ocean (e.g. Campin and Goosse 1999). It can be disguised by applying 'salinity enhancement' near the continental margin of Antarctica. In such attempts the salinity at the surface near the coast is restored to high values in order to mimic the impact of sea-ice formation on the surface salinity and to improve the deep water mass properties. This method has been criticized since the salt flux involved might correspond to sea-ice formation rates much larger than those deduced from observations (Toggweiler and Samuels 1995). The model described here contains a state-of-the-art sea-ice model. It accounts for sea-ice dynamics by solving a two-dimensional momentum equation for the sea-ice velocity which includes interfacial stress at the upper and lower surface of the ice flows and an internal ice resistance to shear and compression based on a viscous-plastic rheology as described by Hibler (1979). Thermodynamically, the sea-ice cover is treated as an insulating two-dimensional slab with linear vertical temperature profile and a salinity corresponding to 5 psu. The insulating property of the ice cover is enhanced by a prognostic snow cover which also changes the surface albedo. Surface melting occurs when the skin temperature rises above melting point. The skin temperature is calculated with a surface heat budget similar to that described by Parkinson and Washington (1979), using near-surface conditions taken from a 15-year integration of the ECHAM4 atmosphere general circulation model (Roeckner et al. 1996). Daily fields are used to account for the non-linear dependence of surface fluxes (and thus deep water formation rates) on the near-surface conditions in the atmosphere. The sea-ice cover is fractional thus accounting for the large differences of heat fluxes over sea-ice and water. Continuity equations are solved for ice thickness, concentration, and snow depth. Outside the ice regions, fluxes of heat, freshwater, and momentum from the same ECHAM4 run are used. The reason for the different treatment of ice and no-ice regions is that ECHAM4 gives better fluxes than bulk formulas. Fluxes, however, cannot be used if ice is present, since the feedback of the ice cover on the heat fluxes is crucial for a stable integration. The forcing is cyclically repeated every 15 years.

A mismatch between the fluxes required by coarse ocean and atmosphere models to simulate a realistic climate requires

additional fluxes of heat and freshwater. These are obtained by restoring the surface salinity and temperature in the ocean to those climatological values that have been used as lower boundary condition in the ECHAM4 integration. The model has a free surface, so that freshwater fluxes can be applied directly without any salt fluxes. Restoring of salinity is achieved by the appropriate freshwater flux. This freshwater flux, however, is not applied in ice regions (defined by monthly observed ice extent), in order to have the salinity changes in the upper ocean exclusively determined by the simulated ice formation and the freshwater fluxes of the atmosphere model. Momentum fluxes are not corrected at all.

The ocean climatology obtained with this forcing is described in Legutke and Maier-Reimer (1999). The model simulates a reasonably realistic annual state and seasonal cycle within the limits given by the grid resolution. The simulated climatology suffers, however, from the described deficiencies of the representation of the downslope descent of dense water. A simple bbl parametrization has now been implemented in the model and a new integration with the bbl included is performed. The results will be compared with the simulation without bbl which is called 'control' experiment.

The approach is similar to the one adopted by Campin and Goosse (1999). The ocean model, however, is different from that of Campin and Goosse (1999) in many respects (horizontal and vertical grid resolution, partial bottom grid cells, parametrization of subgrid-scale mixing, explicit formation of dense water instead of restoring temperature or salinity to extreme values in the formation seasons, inclusion of a sea-ice model).

The bbl parametrization of HOPE-G differs from that of Campin and Goosse (1999) in that it is formulated as a downslope convection similar to the 'slope convection' proposed by Beckmann and Döscher (1997). An exchange of tracer (temperature or salinity) occurs between two horizontally adjacent bottom cells (i.e. cells which would have a common surface if they belonged to the same layer), if the cells belong to different layers and if the higher cell has the higher in situ density at the depth of the upper horizontal surface of the lower cell. The exchange depends on the local geometry. It is proportional to $1/k$, where k is the number of adjacent bottom cells that belong to a lower layer, i.e. the number of potential downslope pathways of the water in the cell in consideration. The exchange is formulated as a diffusion operator using time splitting:

$$\frac{\partial T^{n+1}}{\partial t} = \nabla \cdot (D \cdot \nabla T^n),$$

where T is the bottom value of the tracer, n is the time step, and D depends on the local grid configuration and stratification in the way that the tracer after the exchange is

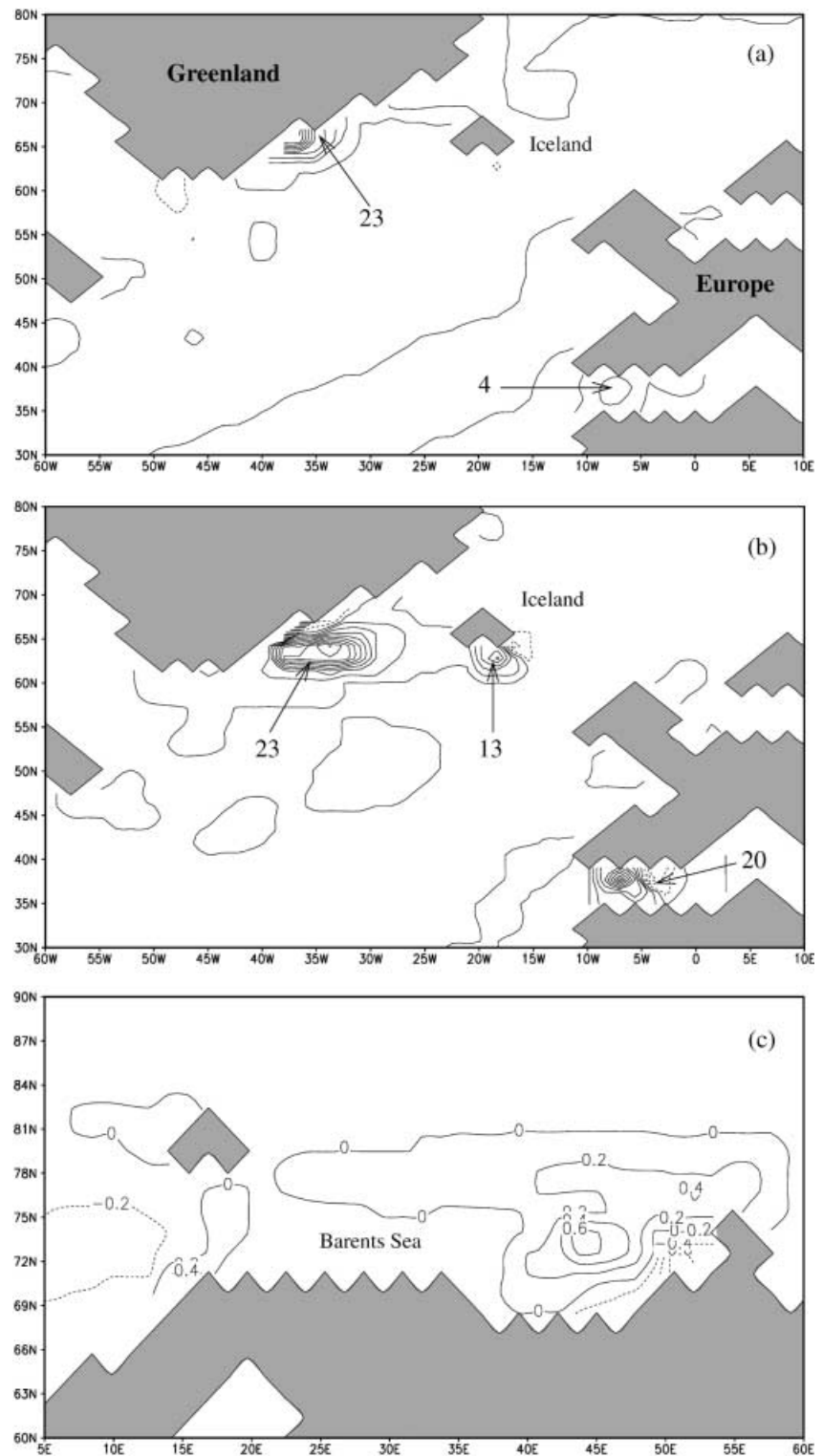
$$T^{n+1} = T^n + \sum_{i=1,4} \delta_i \cdot V^{-1} \cdot \text{Min}(V, V_i) / \text{Max}(k, k_i) \cdot (T_i^n - T^n).$$

V is the cell volume, i is indexing the adjacent cells, and δ_i is set to 0 if the condition for downslope flow are not met, i.e. when the cells are not in different layers or the density in the upper cell is not higher than that of the lower cell at the upper interface of the lower cell. This makes the downslope mixing similar to the formulation of the vertical adjustment process in the model and no new parameter needs to be introduced. The success of the parametrization is evaluated by its overall effect on the model climate, rather than by the accuracy of the representation of the simulated processes. Neglecting the advective aspects of the slope flow and representing it as a directional turbulent process within the bottom cells, it is assumed that the slope flow is of small scale and that the return flow is within the same grid cells. Thereby, ad hoc assumptions on where the return flow takes place are avoided.

It is not checked whether the water parcel can reach its level of neutral density already on a higher level than the next bottom cell, which might be several levels deeper. Thus, only water is mixed downward that would reach the next bottom plateau in the model grid in the absence of entrainment. However, the difference between the number of layers of adjacent columns is larger than 1 in only 3% of all cases.

Both simulations described here have been run for 709 years at which time the change of 15a-mean global temperature is $< 5 \times 10^{-3}$ K and that of global mean salinity $< 10^{-3}$ psu. Both experiments have been started from a state of rest with temperature and salinity stratification taken from the Levitus climatology (Levitus et al. 1994).

Fig. 1. **a** Difference (bbl minus control) of potential energy released by vertical convective adjustment in the North Atlantic. Contour interval is $2.5 \cdot 10^{-3} \text{ W/m}^2$. **b** Change of potential energy caused by the bbl parametrization in the North Atlantic. Contour interval is $2.5 \cdot 10^{-3} \text{ W/m}^2$. Negative contours are *dashed*. **c** Difference (bbl minus control) of potential energy changes caused by total (vertical and downslope) convective adjustment in the Barents and Kara Seas. Contour interval is $0.2 \cdot 10^{-3} \text{ W/m}^2$. Negative contours are *dashed*



3 Results

Slope convection is associated with a change of potential energy in the water columns involved. The global difference pattern of the potential energy change between the control experiment and the experiment including the

bbl parametrization (not shown) reveals that significant changes of downslope and vertical convection are found only in the downstream direction of the Denmark Strait, south of Iceland, in the Strait of Gibraltar, and on the continental margins of the Southern Ocean. These are the regions where significant downslope flow has been observed (Price and O'Neil Baringer 1994).

The vertical convective activity is clearly increased near the southeast coast of Greenland (Fig. 1a). This is a consequence of the downslope convection process, which transports dense bottom water to deeper levels, as indicated by the dipole pattern in Fig. 1b. The change of potential energy resulting from a downslope convection event is negative in the upper cell and positive in the lower cell (besides effects of the nonlinearity of the equation of state and thermobaricity). Downslope convection reduces the vertical stability in the shallower column (e.g. on the shelf). When the water is cooled at the surface, it is more readily mixed with the underlying relatively lighter water. The total volume exchange between Greenland and Scotland is 4.4/–5.7 Sv in/outflow in the bbl experiment, and 4.5/–5.9 Sv in/outflow in the control experiment. Of the latter, 3.9 and –4.2 Sv go through gaps in the ridge between Iceland and Scotland ($1 \text{ Sv} = 10^6 \text{ m}^3 \text{ s}^{-1}$). The net southward flow is due to a northward flow of 1.21 (1.3 Sv) through the Bering Strait and precipitation and continental runoff into the Arctic Ocean in the bbl (control) experiment. There is thus little change of volume transport in this region by the bbl parametrization, in agreement with other studies (Lohmann 1998; Campin and Goosse 1999). The total values of both experiments lie within the range obtained by observations. However, the real outflow seems to be partitioned into equal parts east and west of Iceland (Dickson and Brown 1994). Some vertical convective activity also occurs in the Strait of Gibraltar. However, the absolute values in both experiments, as well as their differences, are small compared to those in other sites (Fig. 1a).

There is some downslope ‘flow’ in the Kara Sea, though with small impact for the potential energy (Fig. 1c). In the depth range 150 m to 400 m in the Arctic Ocean, however, where this downslope convection occurs, the warm temperature bias (ca. 0.5 °C) of the control experiment is reduced by about 40% in the bbl experiment (not shown). At other depths, the temperature profile remained unchanged, as does the salinity profile at all depths. In the deep Norwegian Sea, the difference pattern of the total potential energy change has negative values (Fig. 1c) because of increased stability in the North Atlantic Water (NAW) and reduced vertical convective adjustment in the bbl experiment.

In the control experiment, the regions of most intense vertical mixing activity are the Labrador Sea south of Greenland, the Faeroer Shetland Channel, and the Norwegian Sea (Legutke and Maier-Reimer 1999). The deep water formation rates by vertical mixing there are essentially unchanged by the bbl parametrization (Fig. 1a).

The overall effect of the new parametrization on the salinity and temperature stratification in the central North Atlantic is demonstrated in Fig. 2. The positive temperature error in 1000 m depth is decreased from about 2 °C to 0.75 °C. The salinity error is also reduced by about 50%. These improvements are not only due to

the formation of a fresher deep water mass in the Northern North Atlantic by a larger addition of fresh slope water. A large effect also comes from an improvement of the downslope flow out of the Mediterranean. Without the bbl parametrization, the largest salinity on the Atlantic side of the strait is found at about 800 m depth. With the bbl included, the outflow reaches its level of neutral density near the strait at 1050 m, where it is also found in the observations (not shown). Thus, despite the coarse resolution of the narrow strait, the impact of the deep high-salinity outflow is captured. The exchange through the strait is reduced from 0.86/–0.83 Sv to 0.65/–0.63 Sv. While the values without bbl seem to agree better with observations (Bryden and Kinder 1991), the large scale salinity distribution is better reproduced with the bbl parametrization included (Figs. 2, 3).

The zonal mean salinity differences of the two simulations in the Atlantic Ocean (Fig. 3) is in many aspects similar to the results of Campin and Goosse (1999). Both models show a decrease of salinity (by ca. 0.2 psu) at intermediate depths in the North Atlantic. In HOPE-G, the minimum at 30 °N is due to the modified influence of the Mediterranean water, which is also responsible for the slight increase of salinity at 1450 m depth. The second minimum at 45 °N is due to the larger contribution of fresh Greenland Sea water to the NADW. A significant difference to the results of Campin and Goosse (1999) exists below 2000 m between 30 °N and 60 °N. The freshening in the deep North Atlantic in HOPE-G stems from an increase of AABW inflow from the south which pushes the saltier NADW upwards. The ventilation rate of the deep Atlantic by AABW has increased from about 3 Sv to 4 Sv (not shown) and agrees well with that given by Luyten et al. (1993). In the model of Campin and Goosse (1999) the pattern is similar but with positive sign possibly due to an increase of salinity of the overflow water. In HOPE-G, the overflow water is slightly fresher (Fig. 3).

Both models show a general freshening of the deep Atlantic due to a more efficient ventilation with AABW, and an increase of salinity near the Antarctic continental slope. At this point, however, a model intercomparison is not straightforward. Campin and Goosse (1999) use salinity enhancement near the coast which keeps the shelf salinities at high values independent from other flow characteristics. Increased salinities on the slope in HOPE-G stem from less dilution of brine-enriched shelf water during the downslope descent or increased production of sea-ice, since no relaxation to observed salinities is specified on the Antarctic shelves. The difference pattern of annual mean net ice production (Fig. 4) between the two experiments shows that increased ice production occurs only in the Ross Sea, while in the Weddell Sea the net ice production has decreased due to a stronger inflow of warm shelf water from the east (1.6 Sv, not shown). The net annual sea-ice production at all coastal cells in the Southern Ocean (meridional extent ca. 308 km) is 56 cm in the bbl

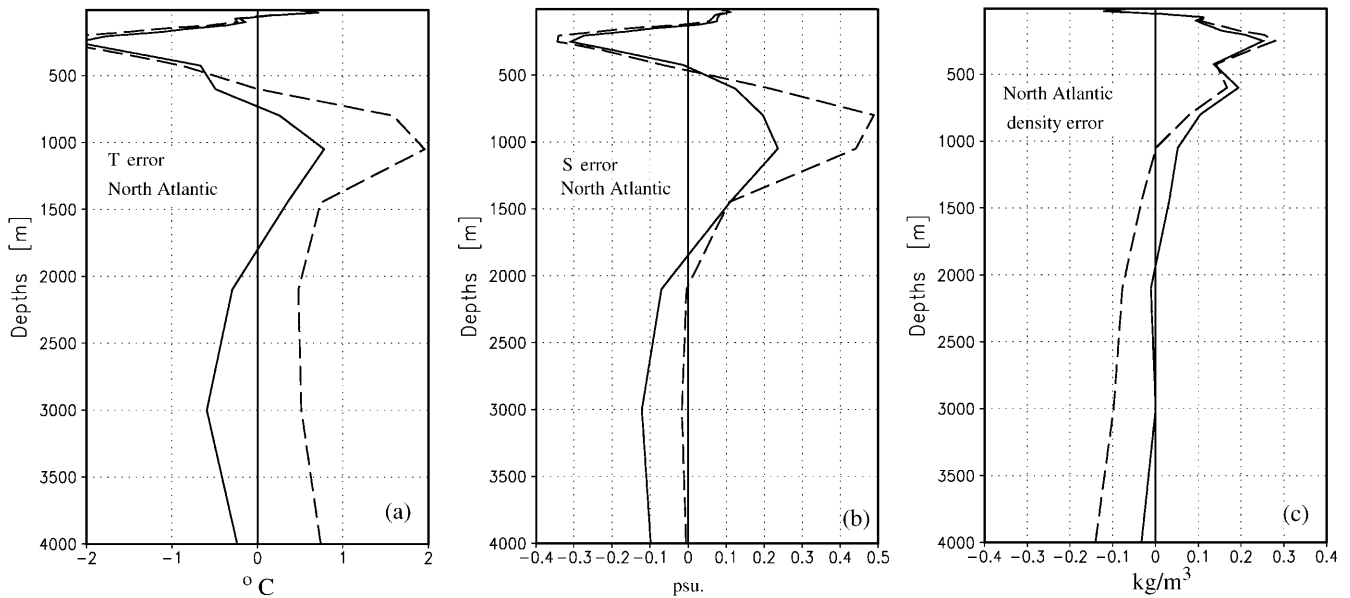
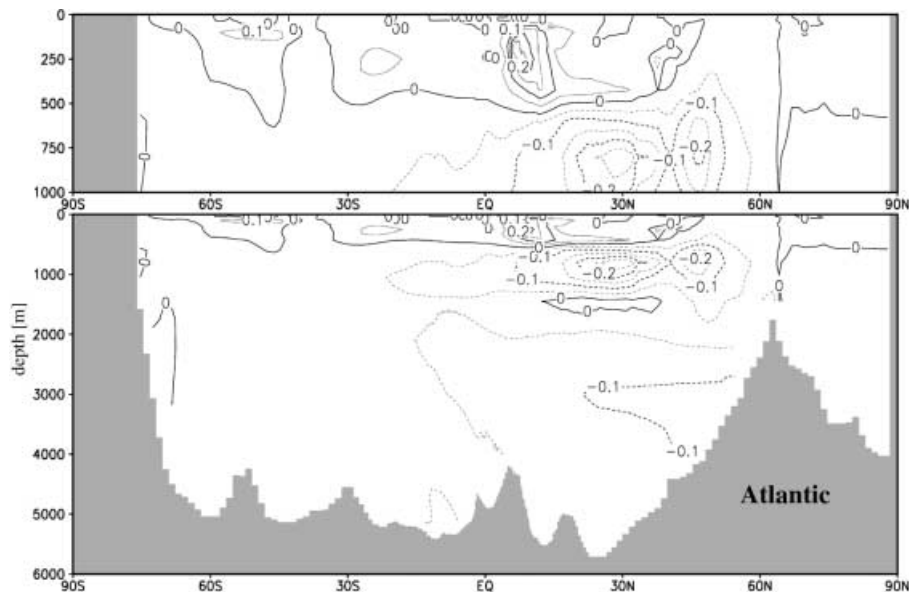


Fig. 2. Simulated vertical profiles of **a** potential temperature ($^{\circ}\text{C}$), **b** salinity (psu), and **c** in-situ density (kg/m^3) error (relative to the Levitus et al. 1994 climatology) in the North Atlantic (areal mean between 46°W and 36°W , and 24°N and 36°N). The *Solid lines* are for the run with the bbl parametrization included and the *dashed lines* for the control run without bbl parametrization

Fig. 3. Difference (bbl minus control) of zonal-mean salinity in the Atlantic Ocean



experiment and 61 cm in the control experiment. Both values are near the formation rates required by the observed salinity budget (Toggweiler and Samuels 1995).

In the Southern Ocean, the differences in convective activity between the bbl and the control experiment show a decrease of vertical convection in the deep water of the Weddell and the Ross Sea, and increased activity in the shallow regions near the coast (Fig. 5a). Similar to the finding southeast of Greenland, this increased vertical coastal convection is a consequence of more efficient downslope transport of dense bottom water when the bbl parametrization is included

(Fig. 5b). The decrease of the spurious deep-reaching open-ocean convection is most obvious in the Ross Sea. In the real world, open-ocean convection in the Southern Ocean is trapped at the surface since the salinity stratification is restored when the newly formed ice is melted by the heat brought convectively to the surface (Martinson 1990). In coarse ocean models, however, open ocean convection often reaches from the surface to some 1000 m down into the CDW layer. This leads to dilution of the deep water by fresh surface water, and thus to a too fresh deep water mass when open ocean convection is strong in the models.

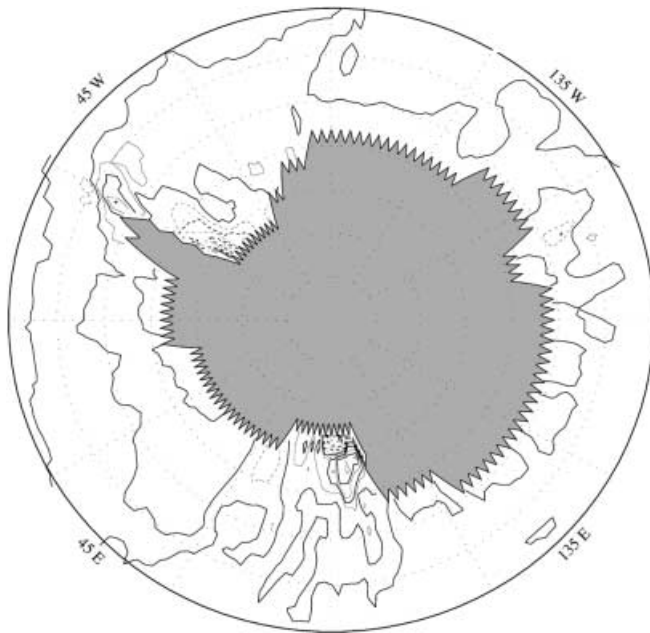


Fig. 4. Difference (bbl minus control) of net sea-ice growth in the Southern Ocean. Contour interval is 20 cm

Figure 6 shows the bottom temperatures in the Weddell Sea. A tongue of very cold water extends from the western slope towards the east. The minimum value of the bbl experiment is near $-1.4\text{ }^{\circ}\text{C}$, almost $1\text{ }^{\circ}\text{C}$ colder than in the control experiment. Maximum values of -0.2 to $-0.4\text{ }^{\circ}\text{C}$ are simulated at the continental break of the eastern Weddell Sea. This pattern compares well with synoptic observations (e.g. Foster and Carmack 1975, their Fig. 13), The bottom salinity, on the other hand, is too fresh by about 0.1 psu and did not change significantly with the bbl scheme. It must be kept in mind, however, that a comparison between different data sets crucially depends on the layer thicknesses used. The temperature maximum in the eastern Weddell Sea is caused by the advection of relatively warm water from the east in the Weddell Sea gyre. This gyre is stronger in the bbl experiment (10%) and suppresses formation of bottom water there. This lack of bottom water formation is in agreement with observation (Fahrbach et al. 1994). The Weddell Sea gyre is convergent above and divergent below 2500 m in both experiments. Below 3500 m, the divergence is 5.5 Sv in the bbl experiment, another 6 Sv divergence is simulated between 2500 m and 3500 m. These values are 5% larger than in the control experiment. The divergence below 3500 m compares well with Weddell Sea Bottom Water formation rates estimated from direct observation (Muench and Gordon 1995). They are smaller than those obtained by Campin and Goosse (1999). However, the divergence in HOPE-G referred to here does not contain the effect of the bbl with is parametrized as a diffusive/convective transport. By contrast, the calculation of Campin and Goosse (1999) who obtained 8 Sv includes the effect of their bbl, which is advective.

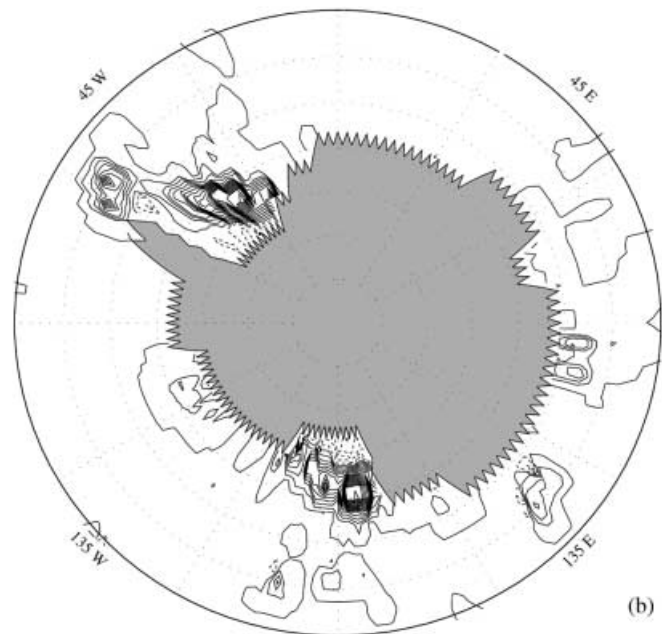
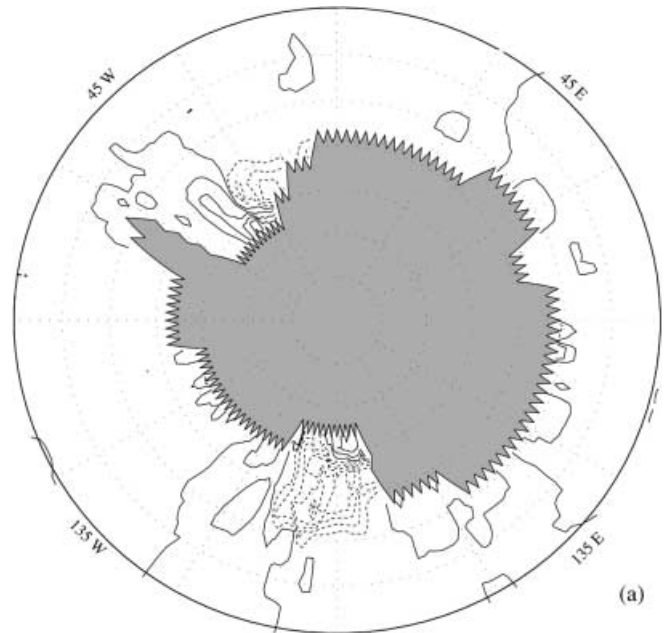
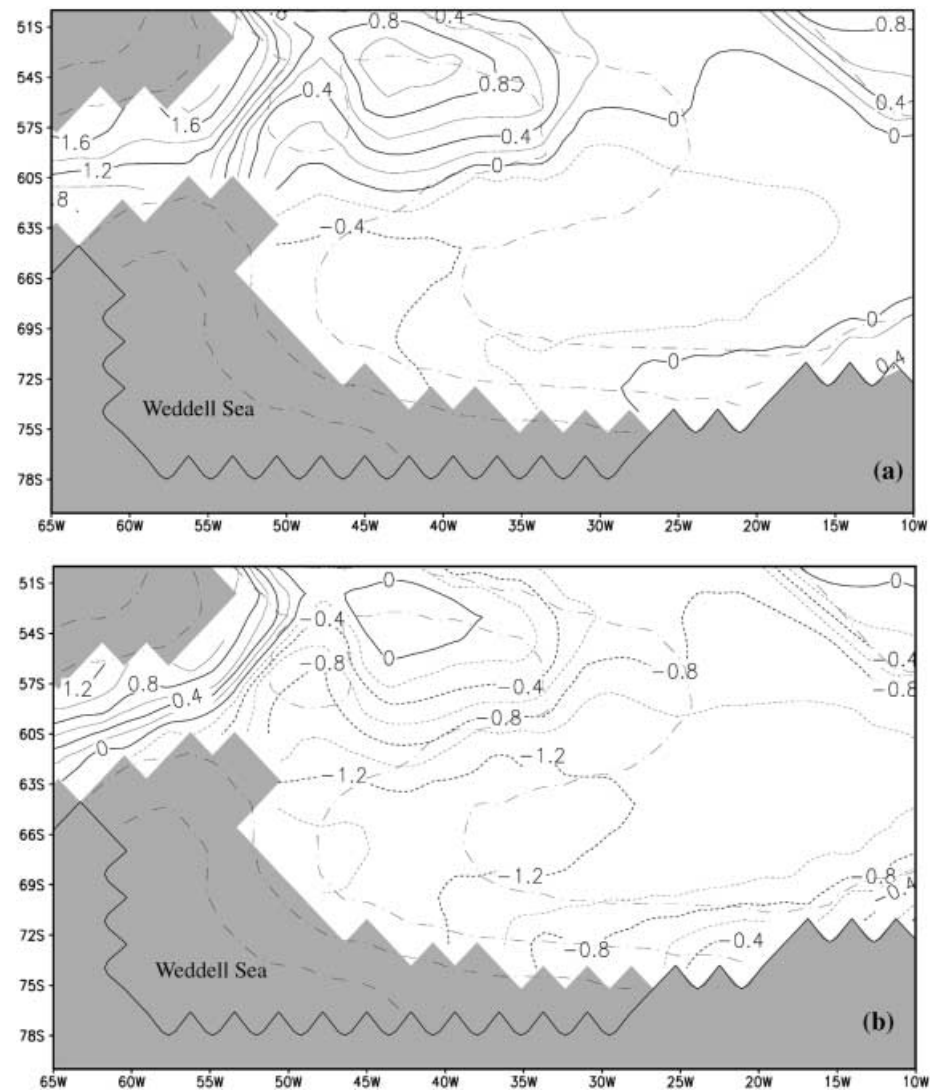


Fig. 5. a Difference (bbl minus control) of potential energy released by vertical convective adjustment in the Southern Ocean. Contour interval is $2.5 \cdot 10^{-3}\text{ W/m}^2$, negative contours are *dashed*. **b** Change of potential energy caused by the bbl parametrization in the Southern Ocean. Contour interval is $2.5 \cdot 10^{-3}\text{ W/m}^2$, negative contours are *dashed*

Figure 7 shows the temperature distribution of both simulations on a meridional transect through the Ross Sea at $175\text{ }^{\circ}\text{E}$. The isotherms of the bbl experiment are sloping with the continental shelf break, as typically obtained from synoptic observations (Muench and Gordon 1995), while in the control experiment they are more horizontally or vertically oriented, depending on whether the water is reached by vertical convection or not. However, the bottom layer is thicker than in the

Fig. 6. Simulated bottom potential temperature (values in lowest grid cell) in the Weddell Sea for depths greater than 2000 m: **a** control reperiment and **b** bbl experiment. Contour interval is 0.2 °C, negative contours are *dashed*. The *dash-dot contours* are bathymetric isolines (C.I. = 1000 m). *Shaded* areas have water depth shallower than 2000 m



observations, since the entire bottom cells belong to the boundary layer in HOPE-G.

Despite the rather large impact of the slope convection on the water mass characteristics, the vertical stream function has not changed much (Fig. 8). The maximum downward transport near 60 °N in the North Atlantic is weakened. However, since the upwelling of NADW between 45 °N and 25 °N is reduced by about the same amount, the outflow of NADW at 30 °S is almost unchanged (10 Sv). With his idealized model of the North Atlantic, Lohmann (1998) also obtained a reduced maximum in the overturning stream function with the ‘slope convection’ included, and no significant reduction of the outflow across the equator. This is in contrast to the result of Campin and Gosse (1999), who obtained a weakened outflow at 30 °S and an essentially unchanged maximum overturning in the North Atlantic. Again, there are differences in the model forcing which complicate a direct comparison with Campin and Gosse (1999). They restore the SST north of 65 °N to climatological winter values all year long. This

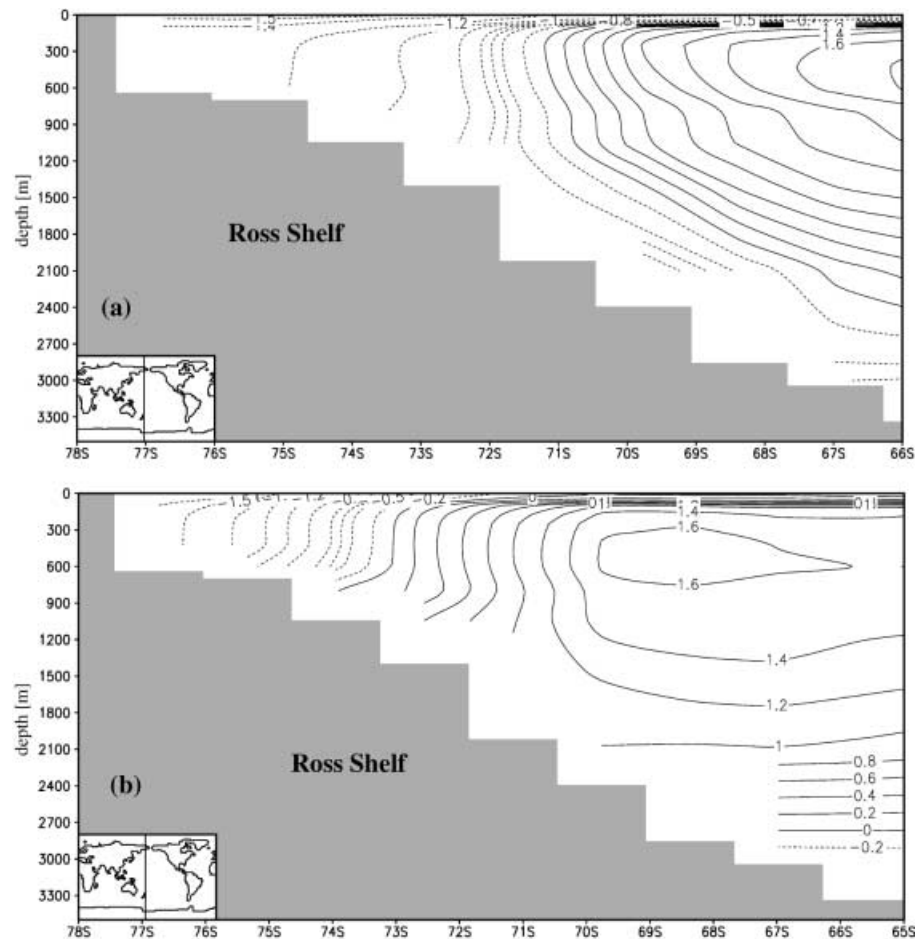
strengthens the deep-water production and the overturning in the North Atlantic.

The formation rate of NADW inferred from observations is 13 to 15 Sv with an addition of 4 to 5 Sv of upwelled AABW. There seems to be a close correspondence of the formation rate and the outflow into the Southern Ocean (Schmitz and McCartney 1993). The upwelling of NADW in the North Atlantic in numerical models is thought to balance spurious horizontal diffusion near the western boundary current (Böning et al. 1995). The reduction of this upwelling and decrease of the ratio of formation and outflow of NADW can be considered as a success of the bbl scheme.

The global Southern Ocean coastal overturning cell is almost unchanged. The seemingly stronger ventilation, if judged from water mass characteristics, is rather due to less dilution of the dense water on its way into the deep ocean than to increased ventilation rates.

Finally, the global density profile is shown in Fig. 9a for both experiments and can directly be compared with that shown by Campin and Gosse (1999). The density

Fig. 7. Potential temperature on a meridional vertical section at 175 °E in the Ross Sea simulated in **a** the bbl experiment and **b** the control experiment. Contour interval is 0.2 °C, negative contours are dashed



in the deep ocean has increased in both models by about the same amount. However, in contrast to the results of Campin and Goosse (1999) it has become slightly larger than the climatological values in HOPE-G. Above 1800 m, Campin and Goosse (1999) show almost no changes caused by their bbl parametrization. In HOPE-G, however, the global density profile has increased at all depths below 700 m which can explain the small changes found in the large scale circulation. More details are seen when anomalies of simulated profiles and the climatology are displayed. In the Pacific Ocean (Fig. 9b), the density anomaly error has increased below 2000 m, in the influence domain of the AABW. This increase is due to a drop of temperature, while the salinity profile is unchanged (not shown). An improvement is obtained below 1500 m in the Indian Ocean (Fig. 9c). These layers are strongly influenced by deep water of Atlantic origin entering the Indian Ocean from the west and profit from the cooler and denser characteristics of the latter.

4 Summary and conclusions

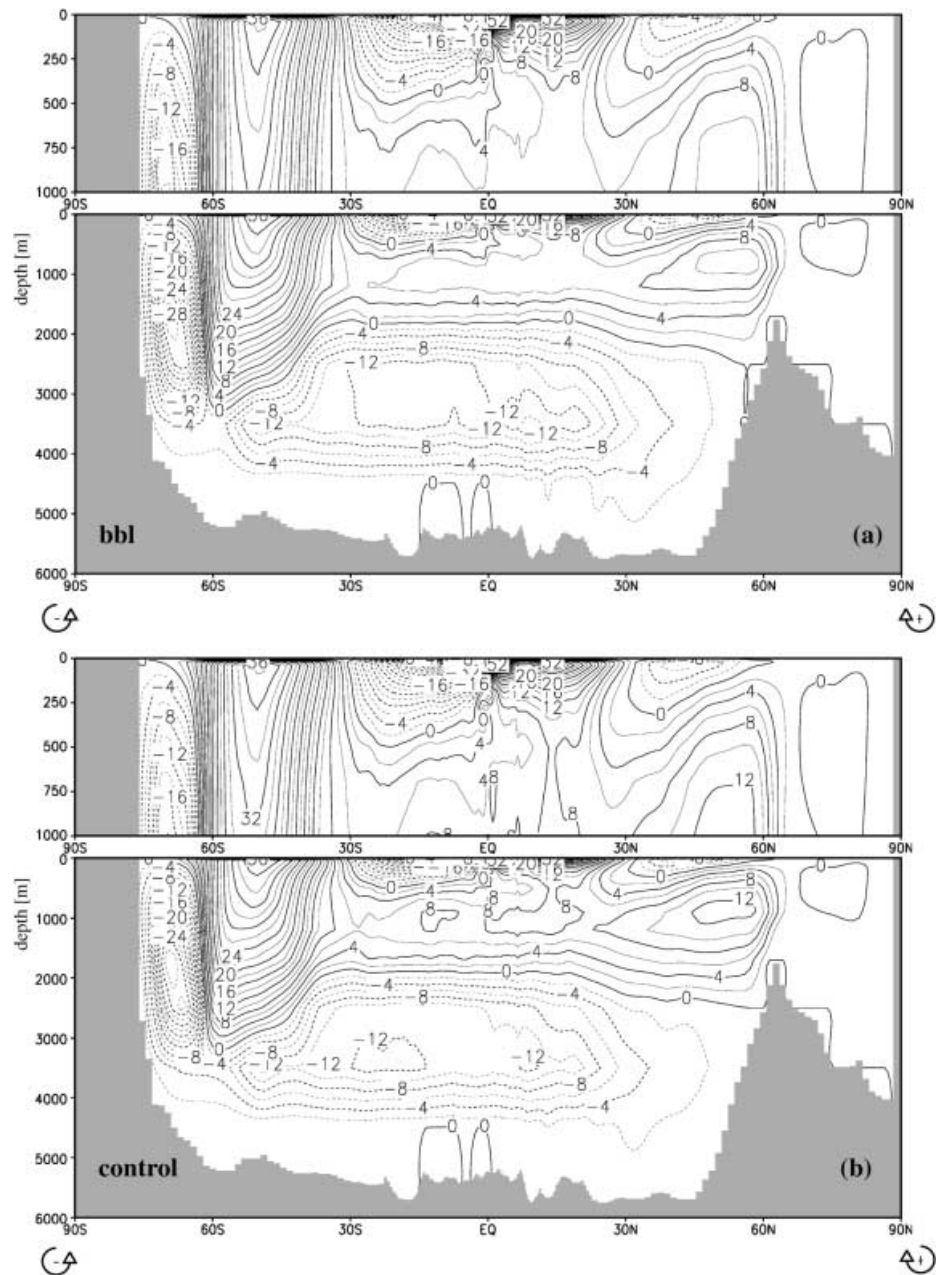
A bbl parametrization scheme has been implemented in a global OGCM with depth-coordinates. The bbl para-

metrization describes the downslope flow as a directional turbulent mixing process, similar to the parametrization of convective overturning of hydrostatically unstable water columns. With regard to the numerous processes involved in downslope flow and their potentially large (and partially counteracting) impact on transport rates, which are not and will not be resolved in the near future in global ocean models, no dependence of the strength of the mixing on the state of the ocean is included. The attraction of the formulation adopted here is by its conceptual simplicity. It does not involve new tunable parameters, it is computationally efficient and easy to implement into existing OGCMs.

Two model versions, with and without the new scheme included, are integrated and their results compared against each other, against observations, and against the results of Campin and Goosse (1999) obtained with a similar study. The locations where downslope transport is simulated by the scheme correspond remarkably well with those where downslope flow is observed directly or indirectly. Wherever downslope flow is simulated, it improves the local water mass characteristics.

The NADW, which is too salty without the scheme, becomes fresher. Also, the Mediterranean outflow finds its level of neutral density at a deeper layer in accord with observations. Another feature which is improved

Fig. 8. Global vertical overturning stream function simulated in the **a** bbl experiment and **b** the control experiment. Contour interval is 2 Sv, negative contours are *dashed*



by the bbl parametrization is the ventilation of the abyssal Atlantic Ocean by AABW from the south. This ventilation is too weak without the scheme and thus the bottom water in the Atlantic Ocean is too warm. However, the dense bottom water formed in the Southern Ocean is too fresh and too cold, so that the strengthened ventilation causes a cold and fresh bias in the water that fills the deepest layers of the Atlantic Ocean.

The water formed on the southern high-latitude shelves can be made more saline by a number of processes. The most important is perhaps the net production of sea-ice. The atmosphere model data, which drive the ocean, are known to give an underestimated heat loss in the Southern Ocean (Roeckner et al. 1996),

so the ice growth rates could be underestimated due to the forcing. The simulated growth rates cannot be compared with direct observations since the latter do not exist. However, if compared with growth rates derived indirectly from salinity budgets on the shelves, they do not appear to be unrealistic, at least near the coast.

With the coarse resolution of the model grid, details of the shelf topography, which are considered important for deep water formation, cannot be resolved. Examples are submarine ridges on the shelf which form pools where the brine rejected during freezing of sea-ice can accumulate. In such pools, water can gain a higher salinity before it spills over the sills near the shelf break.

In z-level coarse-resolution ocean models, open ocean convection, needed to remove static instabilities, is often

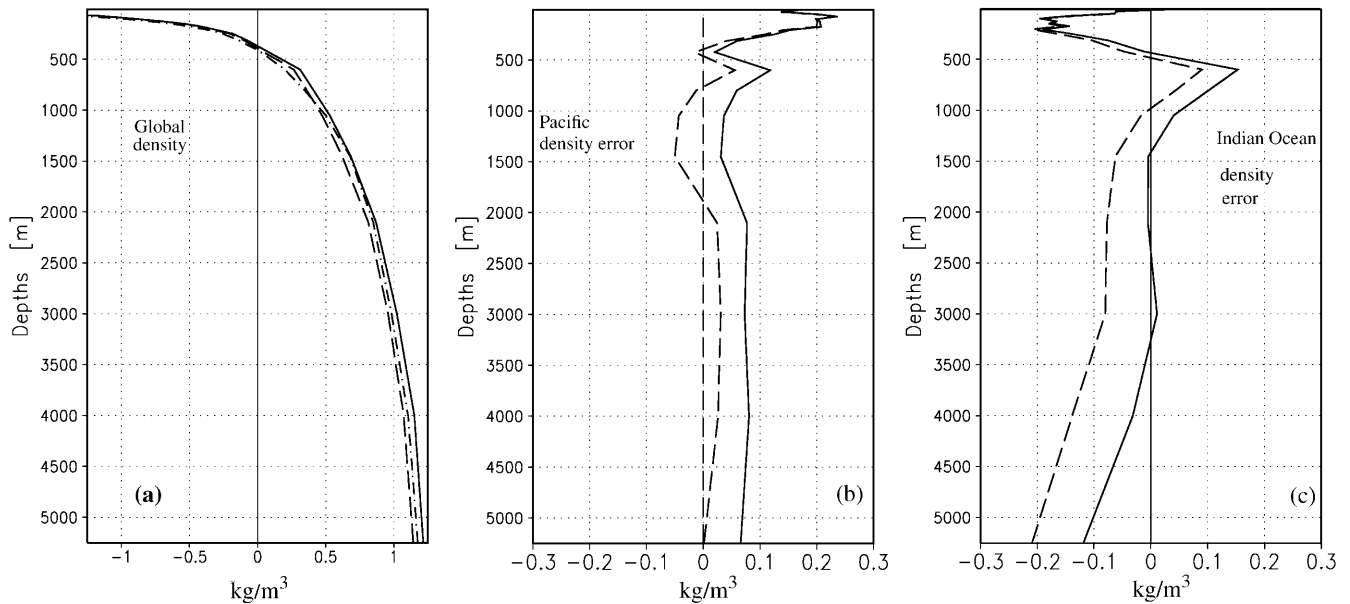


Fig. 9. **a** Global mean vertical profiles of density minus a reference profile calculated with 4 °C and 34 psu. (bbl experiment: *solid line*; control experiment: *dashed line*; Levitus et al. 1994 atlas: *dot-dashed line*) **b** Density error (relative to the Levitus et al. 1994 climatology)

in the **b** Pacific and **c** Indian Ocean. The *solid lines* are for the run with the bbl parametrization included and the *dashed lines* for the control run without bbl parametrization. Units are °C, psu, and kg/m³ respectively

too strong and reaches from the surface into the warm CDW. This process serves as an upward pump of heat and salt, and renders the deep water that flows onto the shelves too cold and too fresh. Consequently, the dense water that is a mixing product of dense shelf and slope water and CDW also becomes too fresh and too cold. The open ocean convection is reduced with the bbl scheme, because the dense shelf water is no longer transported horizontally above lighter water into the open ocean. The slope water formed in the Southern Ocean is more saline. However, since it is still too cold and fresh, the water that settles in the deep ocean can be too fresh, too cold, or both, depending on the ventilation rates.

The bbl scheme does not have a strong impact on the general circulation. It does not strengthen the overturning of NADW. On the contrary, in the North Atlantic, the exchange through straits where downslope flow is simulated is weaker since the pressure gradient is reduced by the downslope transport. Transport values elsewhere are changed by a few per cent only. An exception is the ventilation associated with the Southern Ocean, which is increased from 3 Sv to 4 Sv in the Atlantic and by 0.8 Sv from 9 Sv in the Pacific.

Most of the results are in agreement with other model studies as far as a comparison is possible. The results of these sensitivity studies are confirmed despite a number of differences in the model formulations and the parametrizations of the downslope transport. The impact on the model climatology is similar to that described by Campin and Goosse (1999), the only other long-term simulation we know of, with a global model with realistic topography and a bbl parametrization.

Acknowledgements The experiments have been integrated on a NEC SX-4 in a joint project of MPI and NEC European Supercomputer Systems, NEC Deutschland GmbH. We thank the staff of NEC for their support for keeping the model running. Special thanks are due to Achim Stössel for useful comments on the manuscript.

References

- Aagaard K, Swift JH, Carmack EC (1985) Thermohaline circulation in the Arctic Mediterranean Sea. *J Geophys Res* 90: 4833–4846
- Adcroft A, Hill C, Marshall J (1997) Representation of topography by shaved cells in a height coordinate ocean model. *Mon Weather Rev* 125: 2293–2315
- Baines PG, Condie S (1998) Observations and modeling of Antarctic downslope flow: a review. Jacobs SS, Weiss RF Ocean, ice, and atmosphere: interactions at the Antarctic continental margin. Am Geophys Union, Washington DC, pp 29–49
- Beckmann A, Döscher R (1997) A method for improved representation of dense water spreading over topography in geopotential-coordinate models. *J Phys Oceanogr* 27: 581–591
- Böning CW, Holland WR, Bryan FO, Danabasoglu G, McWilliams JC (1995) An overlooked problem in model simulations of the thermohaline circulation and heat transport in the Atlantic Ocean. *J Clim* 8: 515–523
- Bryden H, Kinder TH (1991) Steady two-layer exchange through the Strait of Gibraltar. *Deep-Sea Res* 38: 5445–5463
- Campin JM, Goosse H (1999) parametrization of density-driven downsloping flow for a coarse-resolution ocean model in z-coordinate. *Tellus* 41A: 412–430
- Danabasoglu G, McWilliams CJ (1995) Sensitivity of the global ocean circulation to parametrizations of mesoscale tracer transports. *J Clim* 8: 2967–2987
- Dickson RR, Brown J (1994) The production of North Atlantic Deep Water: sources, rates, and pathways. *J Geophys Res* 99(C6): 12,319–12,341

- Drijfhout SS, Heinze C, Latif M, Maier-Reimer E (1996) Mean circulation and internal variability in an ocean primitive equation model. *J Phys Oceanogr* 26(4): 559–580
- England MH (1993) Representing the global-scale water masses in ocean general circulation models. *J Phys Oceanogr* 23: 1523–1552
- Fahrbach ER, Peterson G, Rohardt G, Schlosser P, Bayer R (1994) Suppression of bottom water formation in the southeastern Weddell Sea. *Deep-Sea Res* 41(2): 389–411
- Foster TD, Carmack E (1976) Frontal zone mixing and Antarctic Bottom Water formation in the southern Weddell Sea. *Deep-Sea Res* 23: 301–317
- Frey H, Latif M, Stockdale T (1997) The coupled GCM ECHO-2. Part I: the tropical Pacific. *Mon Weather Rev* 125(5): 703–720
- Hibler III WD (1979) A dynamic thermodynamic sea ice model. *J Phys Oceanogr* 9: 815–846
- Jungclaus JH, Mellor GL (1999) A three-dimensional model study of the Mediterranean outflow. *J Mar Sys* 651
- Killworth PD, Edwards NR (1999) A turbulent bottom boundary layer code for use in numerical models. *J Phys Oceanogr* 29: 1221–1238
- Legutke S (1991) Numerical experiments relating to the “Great Salinity Anomaly” of the seventies in the Greenland and Norwegian seas. *Progr Oceanogr* 17: 341–363
- Legutke S, Maier-Reimer E (1999) Climatology of the HOPE-G global ocean general circulation model. Tech Rep 21, German Climate Computer Centre (DKRZ), Hamburg, 90 pp (<http://www.dkrz.de/dkrz/dkrz99.html#PUB>)
- Legutke S, Maier-Reimer E, Stössel A, Hellbach A (1997) Ocean-sea-ice coupling in a global general circulation model. *Ann Glaciol* 25: 116–120
- Levitus S, Burgett R, Boyer TP (1994) World Ocean Atlas, vol 3, salinity and vol 4, temperature. NOAA Atlas NESDIS 3/4, U. S. Government Printing Office, Washington, DC, USA
- Lohmann G (1998) The influence of a near-bottom transport parametrization on the sensitivity of the thermohaline circulation. *J Phys Oceanogr* 28: 2095–2103
- Luyten J, McCartney M, Stommel H (1993) On the sources of North Atlantic Deep Water. *J Phys Oceanogr* 23: 1885–1892
- Marsland SJ, Wolff J-O (2001) On the sensitivity of Southern Ocean sea ice to the surface freshwater flux: a model study. *J Geophys Res* 106(C2): 2723–2741
- Martinson DG (1990) Evolution of the Southern Ocean winter mixed layer and sea ice: open ocean deepwater formation and ventilation. *J Geophys Res* 95(C7): 11 641–11 654
- Muench RD, Gordon AL (1995) Circulation and transport of water along the western Weddell Sea margin. *J Geophys Res* 100: 18,503–18,515
- Parkinson CL, Washington WM (1979) A large-scale numerical model of sea ice. *J Geophys Res* 84(C1): 311–337
- Price JF, O’Neil Baringer M (1994) Outflows and deep water productions by marginal seas. *Progr Oceanogr* 33: 161–200
- Price JF, O’Neil Baringer M, Lueck RG, Johnson GC, Ambar I, Parilla G, Cantos A, Kennelley MA, Sanford TB (1993) Mediterranean mixing and dynamics. *Science* 159: 1277–1282
- Reid JL (1979) On the contribution of the Mediterranean outflow to the Norwegian-Greenland Sea. *Deep-Sea Res* 26: 1199–1223
- Rhein M, Hinrichsen HH (1993) Modification of Mediterranean water in the Gulf of Cadiz, studied with hydrographic, nutrient, and chlorofluoromethane data. *Deep-Sea Res* 40: 267–291
- Rintoul SR (1998) On the origin and influence of Adelie Land Bottom Water. In: Jacobs SS, Weiss RF (eds) *Ocean, ice, and atmosphere: interactions at the Antarctic continental margin*. Antarctic Research Series, Washington DC, pp 151–171
- Roeckner E, Arpe K, Bengtsson L, Christoph M, Claussen M, Dümenil L, Esch M, Giorgetta M, Schlese U, Schulzweida U (1996) The atmospheric general circulation model ECHAM-4: model description and simulation of present-day climate. Rep Max-Planck-Institute, Hamburg, 218, 90 pp (<http://www.mpi-met.mpg.de/deutsch/Sonst/Reports/index.html>).
- Schauer U, Muench RD, Rudels B, Timokhov L (1997) Impact of eastern Arctic shelf waters on the Nansen Basin intermediate layers. *J Geophys Res* 102: 3371–3382
- Schmitz WJ, McCartney MS (1993) On the North Atlantic circulation. *Rev Geophys* 31(1): 29–49
- Song YT, Chao Y, (2000) An embedded bottom boundary layer formulation for z-coordinate models. *J Atmos Oceanic Technol* 17(4): 546–460
- Stössel A, Kim SJ (1998) An interannual Antarctic sea-ice - ocean mode. *Geophys Res Lett* 25(7): 1007–1010
- Toggweiler JR, Samuels B (1995) Effect of sea ice on the salinity of Antarctic Bottom Waters. *J Phys Oceanogr* 25: 1980–1997
- UNESCO (1983) Algorithms for computation of fundamental properties of sea water. UNESCO Technical Papers in Marine Science, 44
- Wolff J-O, Maier-Reimer E, Legutke S (1997) The Hamburg Ocean Primitive Equation Model. Tech Rep 13, German Climate Computer Center (DKRZ), Hamburg, 98 pp (<http://www.dkrz.de/dkrz/dkrz99.html#PUB>)